Deep-Water Traction Current in Upper Carboniferous Stratigraphic Succession of Moscow Stage, Southeastern Pre-Caspian Basin

Yajun Zhang [1], Hansong Dai [1], Huizhen Zhang [1] and Ling Guo [2],*

1   Research Institute of Petroleum Exploration and Development-Northwest, PetroChina, Lanzhou 730020, China; zhang_yj@petrochina.com.cn (Y.Z.)
2   State Key Laboratory of Continental Dynamics, Department of Geology, Northwest University, Xi'an 710069, China
*   Correspondence: guoling@nwu.edu.cn

Abstract: Deep-water currents are geographically widespread and represent important tight-oil and -gas reservoirs. However, identifying deep-water traction current deposits is challenging work. The main objectives of this research were to identify a new type of reservoir deposited in deep-water traction currents. Based on high-quality 3D seismic data and drilling data (logging data and lithology), the sedimentary characteristics of the MKT Formation of the upper Carboniferous Moscow Stage, southeastern Pre-Caspian Basin, were determined. The MKT Formation of the upper Carboniferous Moscow Stage is mainly composed of mudstone and some thin-bedded siltstone. This formation contains a series of "reversal foresets" dipping west (early paleo–high provenance during the depositional stage). Based on the seismic data and drilling logging data, lithology, paleo-geographic position, seismic facies, and form and scale, deep-water traction current deposits were identified in the M block. The discovery of deep-water traction current deposits in the M block not only provides a precious example for research on Paleozoic deep-water traction current deposits, and enriches our knowledge of basin sedimentary types, but also proves that the M block had complex fluid features and unveils a new domain for petroleum exploration in the basin.

Keywords: siliciclastic depositional environment; hydrocarbon reservoirs; reversal foreset; deep-water traction current; Pre-Caspian Basin

1. Introduction

The MKT Formation in the upper Carboniferous Moscow Stage of the M block contains substantial mudstone, serving as the primary cap rock for the Carboniferous petroleum system in the southeastern Pre-Caspian Basin. During deposition, the MKT Formation consisted of a sequence of "reversal foresets" that dipped westward towards the paleo-uplift [1]. The absence of a definitive explanation for this sedimentary configuration leads to significant controversy surrounding the understanding of the overall sedimentary evolution of the Carboniferous System in this region. In the realm of oil and gas exploration, deep-water mudstone layers are predominantly considered to be either source rock or cap rock [2–5]. However, studies focusing on their sedimentary configurations are scarce, and the prevailing consensus suggests their widespread occurrence in sheet-like or horizontally layered formations. The sedimentary history of the upper Carboniferous in the southeast margin of the Pre-Caspian Basin, particularly within our study area, remains relatively under-studied.

Pu et al. (2012) found that deep-water mudstone deposited in the distal part of a pre-delta had a "foreset" configuration [6]. However, this differs from the 'reversal foreset' observed in the MKT Formation. McConnico and Bassett (2007) indicated that

depositional processes on the foresets along the Conway Coast and presumably all Gilbert-type fan deltas, New Zealand, were dominated by sediment gravity flows originating from hyperpycnal river flow and gravity-induced slumps [7]. Research conducted by Shanmugam (2003) identified deep-marine tidal bottom currents and their reworked sands in modern and ancient submarine canyons [8], while Wang et al. (2018) detailed the sedimentological and geological characteristics of the middle Ordovician Yingtaogou Formation, recognizing it as a mixed turbidite–contourite system situated on the western margin of the North China Craton [9]. Additionally, Gong et al. (2015) identified bottom-current reworked sands lacking typical turbidite signatures, suggesting their formation by bottom currents in the northeastern South China Sea [10].

The "reversal foreset" configuration of fine sediments is common in deep-water traction current deposits and is a typical mark of such deposits [11]. The present study conducted a comprehensive analysis and juxtaposition of the "reversal foreset" arrangement found in the MKT Formation against standard deep-water traction current deposits. This comparison encompassed evaluations across various aspects such as lithology, sedimentary context, seismic facies, morphology, and scale, among other factors, aimed at discerning commonalities and elucidating their sedimentary attributes. On this basis, the large-scale "reversal foreset wedge" at the top of the deep Visean Formation (without well data) was also examined to speculate its possible genesis.

The primary goal of this research is to provide an overview of the seismic data and propose a comprehensive sedimentary model for the MKT Formation (upper Carboniferous Moscow Stage) located in the southeastern margin of the Pre-Caspian Basin. Given that this formation holds hydrocarbon reserves in various areas, including the Zanarol uplift, Temel uplift, and southeast depression belt within the southeastern margin of the Pre-Caspian Basin [12], our proposed sedimentary model aims to aid in identifying potential reservoir/seal intervals within this region.

The main goal of our investigation is to reconstruct the sedimentary history of our study area. By conducting a comparative analysis of our sedimentary system reconstruction with previously published works, through our findings, we aim to contribute to the comprehension of the paleoenvironment and stratigraphy during the upper Carboniferous period in the region.

2. Geological Setting

The Pre-Caspian Basin is a large Paleozoic basin located at the junction of the Earasian continent and west of Kazakhstan [13] (Figure 1A). The M block is in the east of the Astrakhan–Aktobe uplift zone in the southeastern region of the Pre-Caspian Basin (Figure 1B). During the late Devonian to the early Carboniferous, the Pre-Caspian Basin served as the passive margin of the East European craton [14]. Subsequently, from the early Carboniferous to early Permian, it transformed into a significant equatorial sag basin due to the collision between the Kazakhstan and East European plates. This evolution led to the formation of a deep-water central depression and uplifted fold belts along the southern and eastern margins [15]. In the late Carboniferous, two distinct lithofacies were deposited: organic-rich shales within the intra-shelf basin of the central Pre-Caspian depression and shallow marine carbonates on the structural highs of the Astrakhan–Aktobe uplift zone at the southeastern margin (Figure 1B) [14].

The Zanarol uplift, predominantly a carbonate ramp during the late Cisean–Gzhelian stage [16], was situated on the Astrakhan–Aktobe uplift zone in the southeastern margin of Pre-Caspian Basin (Figure 1B). Within the Zanarol uplift, the carbonate reservoir of the M block is stratigraphically divided into two formations, KT-II (lower Moscovian) and KT-I (upper Moscovian), separated by the middle Moscovian terrigenous interval known as the MKT Formation, corresponding to a significant transgression event (Figure 2) [14].

The MKT Formation represents deeper-water deposits found within the deep-water shelf-slope facies that formed during the middle Moscovian period of the late Carboniferous (Figure 2). This formation predominantly consists of shale [17] and is composed of thick

mudstone interbedding with thin fine-silty sandstone, limestone, and some sandstone (Figure 2). Based on statistics, the MKT Formation comprises approximately 60–95% mudstone content, averaging around 78%. Vertically, the MKT Formation exhibits abrupt contact at its base with the KT-II limestone, while its upper boundary transitions more gradually into the KT-I limestone, featuring a series of transitional facies deposits spanning 20–50 m in thickness. Spanning approximately 2500 km^2, this formation displays a thinning trend from east to west, presenting as a slope belt that is higher in the east and gradually descends towards the west across the region (Figure 1B). Based on regional data, it is indicated that during the Moscovian period of the late Carboniferous, the southeastern margin of this basin underwent a transition from a passive continental margin to a back-arc basin. The paleo-landform demonstrated a higher elevation in the western region and a lower elevation in the eastern area during this period. The significant Ural orogeny at the end of the Permian resulted in considerable tectonic uplift and inversion, specifically on the eastern side of the basin [18–21]. Hence, the westward-dipping "foreset layers" observed within the MKT Formation contradict the late Carboniferous paleo-tectonic direction and characterize a typical "reversal foreset" configuration.
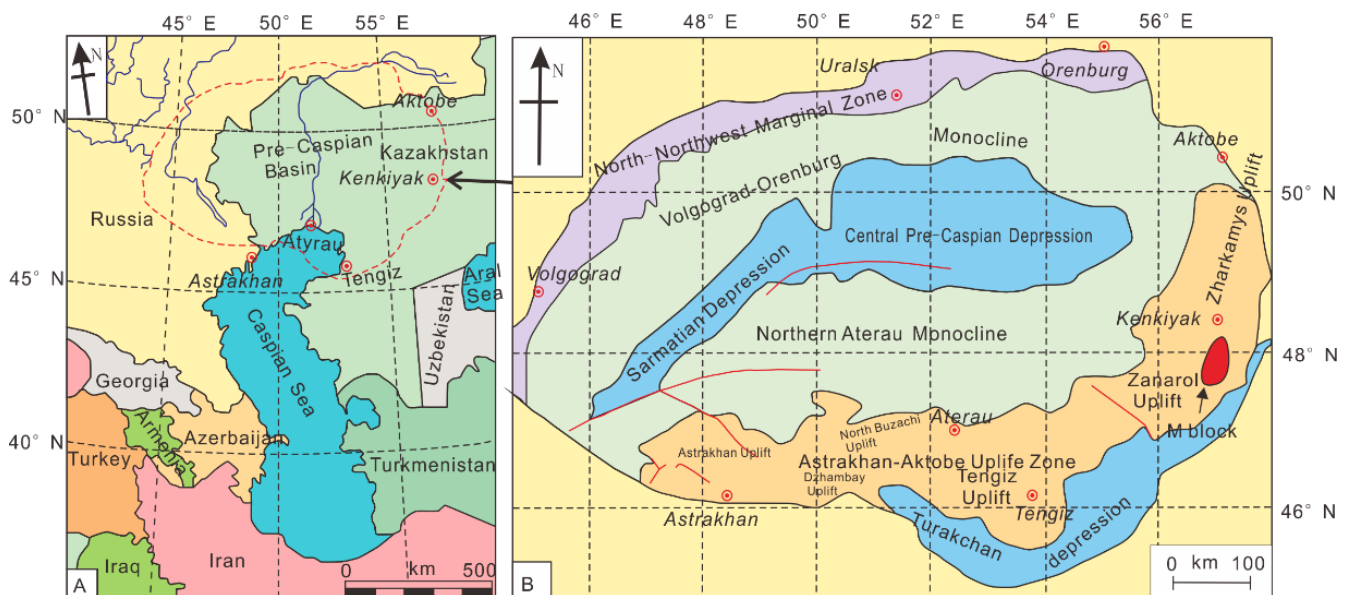

Figure 1. (**A**) Location map of Pre-Caspian Basin in Eurasia. The contour of the Pre-Caspian Basin is marked by a red dotted line (modified after [14,22]). (**B**) Division of the geological structure in the Pre-Caspian Basin. The location of the M block is marked by a red ellipse.
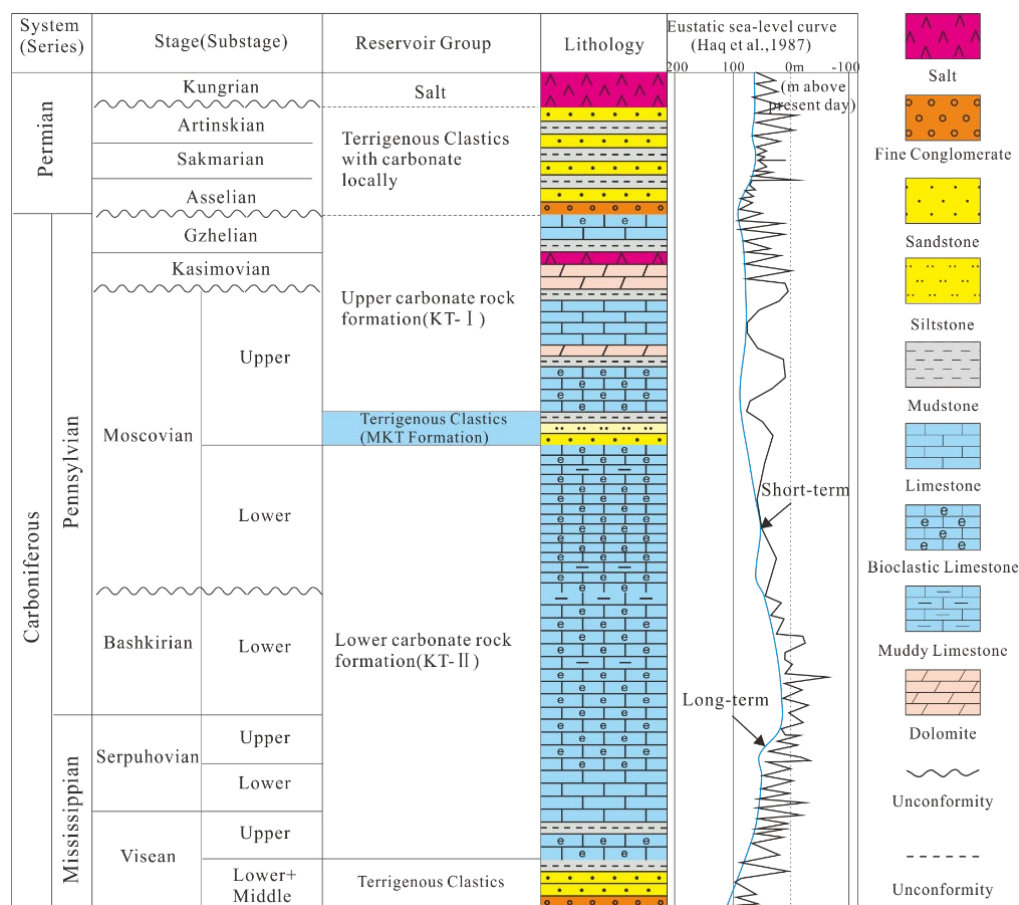
Figure 2. Stratigraphic column of Carboniferous at Zanarol uplift in Pre-Caspian Basin [23] with global sea-level curve proposed by [14,24].

3. Materials and Methods

The data used in this study were obtained from PetroChina. The well data include wire-line logs (conventional raw data, gamma ray, resistivity, neutron, and density measurements). Additionally, supplementary materials such as lithology profiles and seismic profiles from other typical deep-water traction current deposits were acquired from previously published literature.

The study methodology primarily involved deducing seismic correlations and interpreting seismic sections to conduct a sedimentary system analysis. The seismic data analyses included reflector picking, reflector identification, and their correlation; closing loops; fault location; isochronous, constructing cross-sections; and structural contour maps. The flattened surface is the top of the Visean, where this surface is characterized by marked changes in petrophysical properties. Some traced reflectors were selected to show the structural pattern and stratigraphic characteristics in the area.

This approach relied on comparing the MKT Formation in the M-block of the southeastern Pre-Caspian Basin with typical deep-water traction current deposits from various aspects. Firstly, single-well sedimentary facies were analyzed in terms of the paleogeography, water setting, and lithological features to initially assess the depositional environment of the MKT formation. Subsequently, seismic interpretation was employed to elucidate the structural morphology, distribution characteristics, and scale of seismic facies within the MKT formation. Lastly, the depositional mechanism of the MKT formation was analyzed, and a deep-water traction current model was established for the MKT formation in the M block.

4. Results

4.1. Sedimentary Characteristics of MKT Formation

The MKT Formation within the M block primarily comprises gray and black shale, along with interbedded thin-bedded siltstone, muddy siltstone, and limestone. The black and gray shale layers, spanning from 150 to 450 m, are predominantly deposited in deep-water shelf environments (Figure 3). Notably, thin-layered siltstone with thicknesses from 1 m to 5 m, exhibiting a finger-shaped gamma-ray (GR) logging curve, is interpreted as being indicative of contour current activity. They are interbedded with gray, dark-gray, and black shale deposited in the deep-water shelf. In the continuous well section, the deep gray shale is distributed in thick layers and extends extensively laterally. Contour currents are primarily distributed in a lens-shaped formation, with a limited lateral extent and thin thickness (Figure 4).
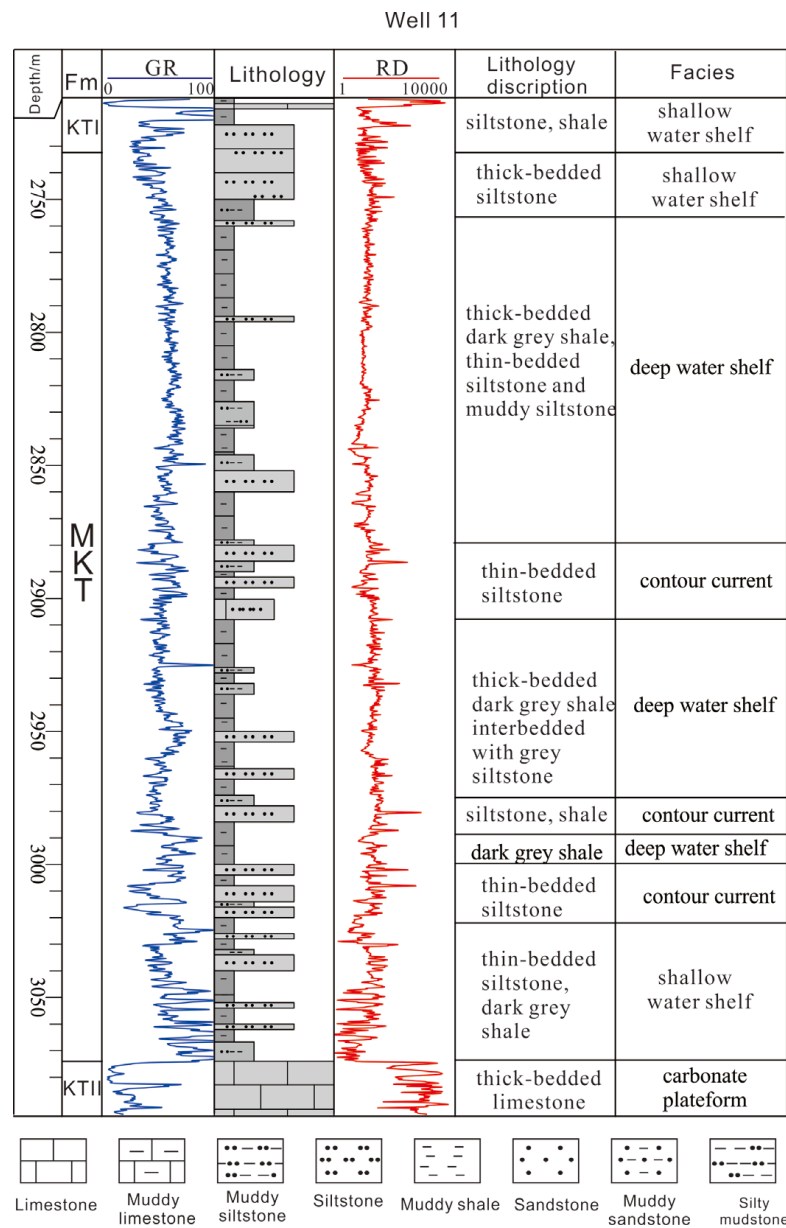

Figure 3. Lithofacies and sedimentary facies of MKT Formation in Well 11 (location of Well 11 is shown in Figure 5B). Fm—formation, KTII—lower carbonate rock formation (see Figure 2), MKT formation—Terrigenous clastics (see Figure 2), KTI—upper carbonate rock formation (see Figure 2).
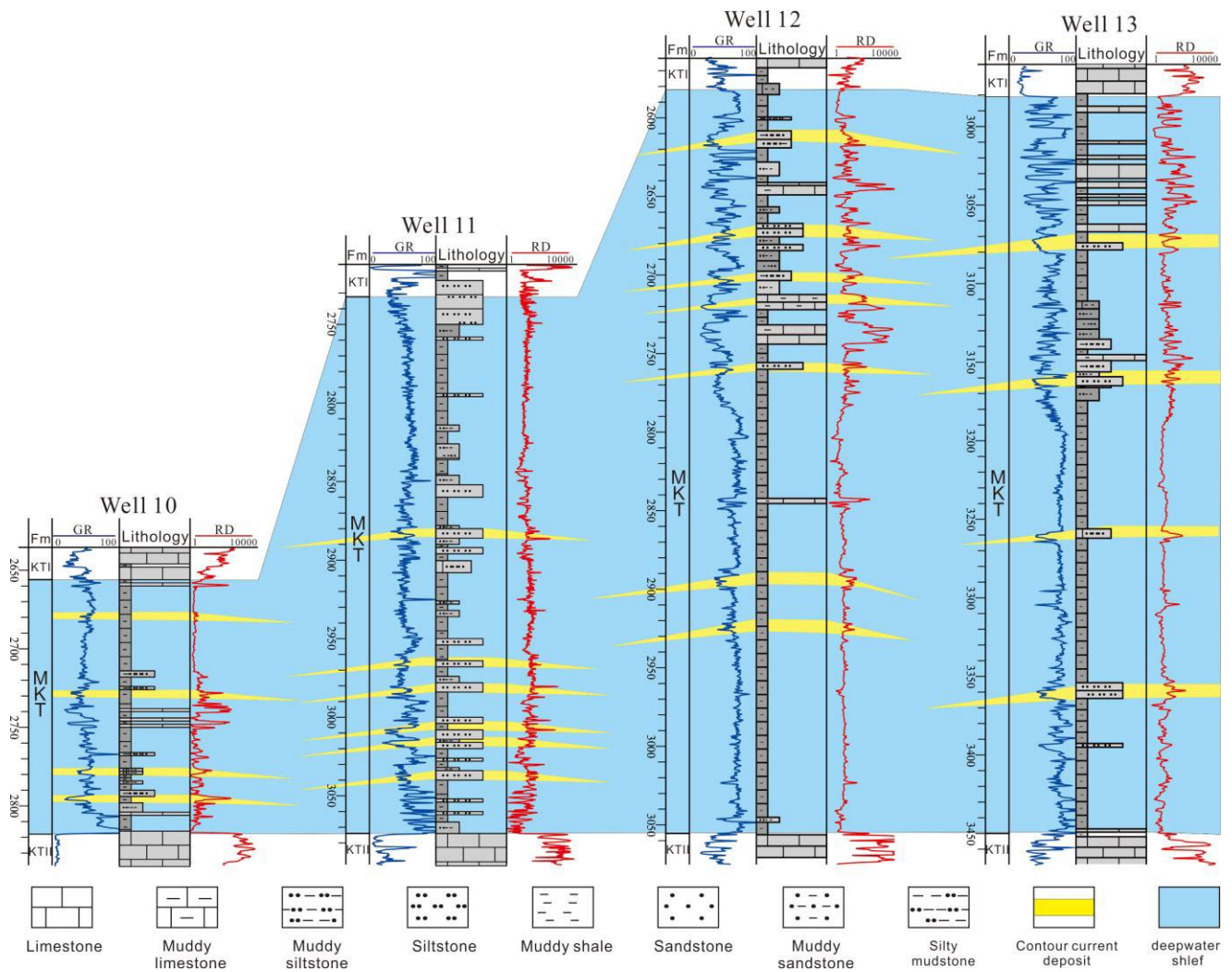
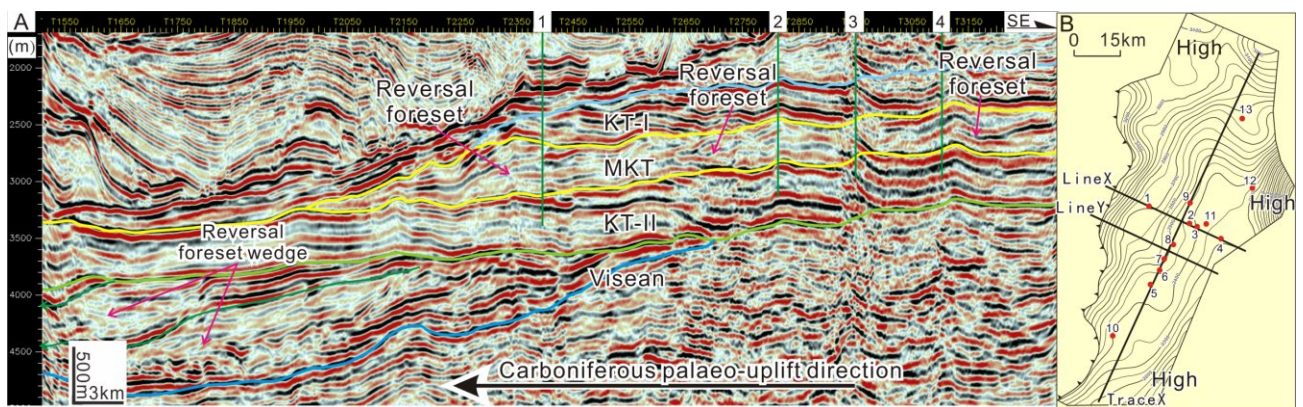**Figure 4.** Sedimentary facies comparison map of MKT Formation in study area.

Figure 5. Interpretation of LineX (**A**) and structure map of MKT top and well locations (**B**) in the study area.

4.2. Characteristics of MKT Formation in 3D Seismic Profile

The thickness of the MKT Formation exhibits a trend of increasing thickness towards the southeast and manifests a distinctive "reversal foreset" configuration in the 3D seismic profiles within the study area (Figure 5). The strata primarily consist of shale, interspersed with layers of siltstone, as illustrated in Figure 3. Notably, there is no observable correlation between the "reversal foreset" configuration and lithology in deep-water traction current deposits. The "foresets" within the interval wave were found to be uniformly distributed across mudstone and clastic rock intervals in the middle–upper Ordovician [18]. The "reversal foresets" observed in the MKT Formation exhibit similar characteristics. The cross-well sections illustrate the presence of "foresets" in both mudstone and non-mudstone sections (Figure 6A). Additionally, the "reversal foreset" displays significant lateral variation in seismic facies characteristics, suggesting considerable lithological instability (Figure 6B,C).
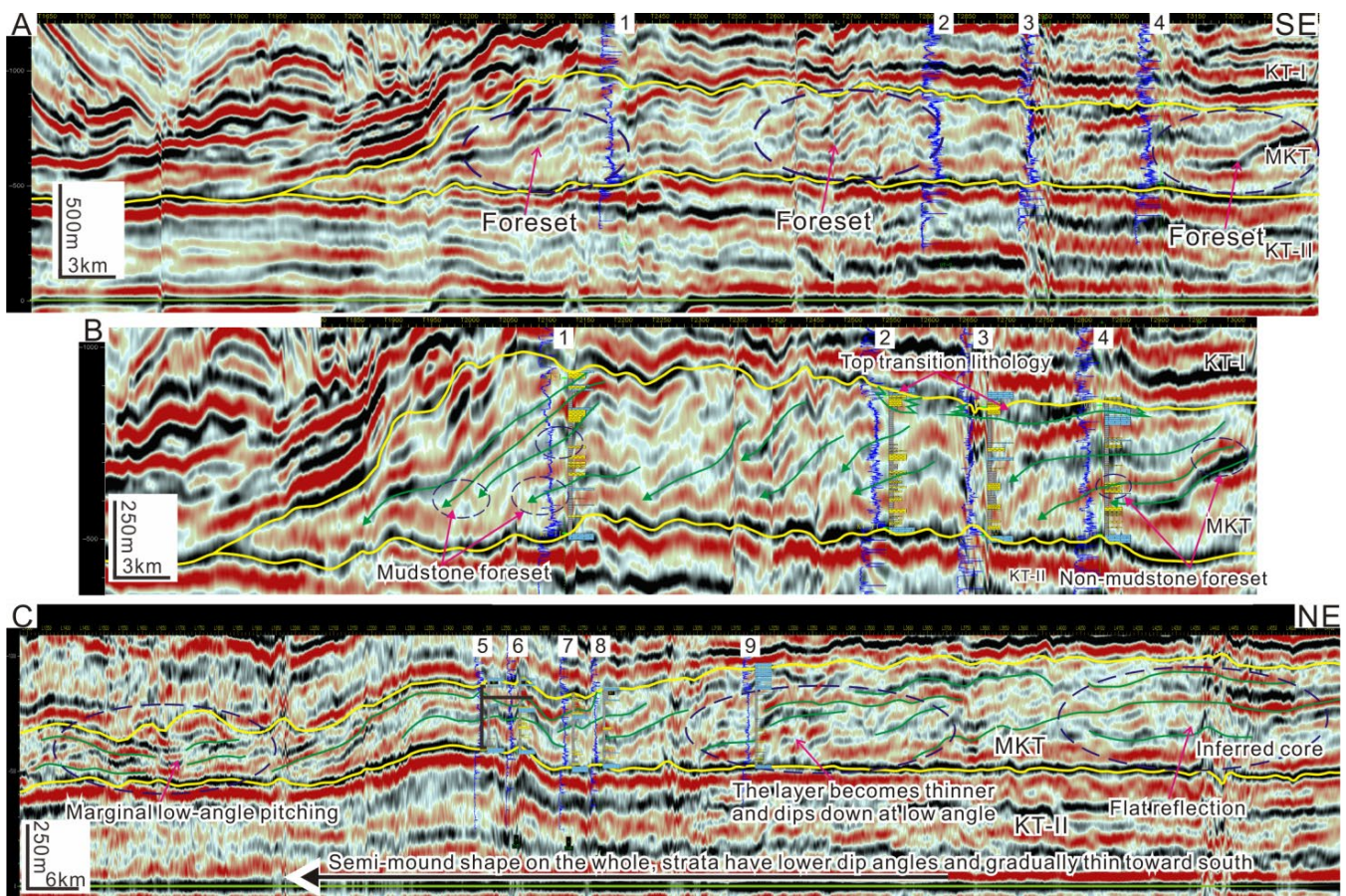

Figure 6. Flattened Visean top sections of LineX (**A**,**B**) and TraceX (**C**). The section's location is shown in Figure 5B.

The internal distribution of strata within deep-water traction current deposits is typically parallel to the tectonic line, primarily influenced by the nature of the water body. For instance, examples such as the "reversal foresets" found in bathymetric lithoherms in Canterbury, New Zealand, the internal wave deposits in the middle–upper Ordovician period in the Tazhong area, and the bathymetric lithoherms in the Miocene period in Finney, Ireland, all exhibit alignment parallel to the tectonic line within the slope zone [18,25–27]. The NE-SW striking orientation of the "reversal foresets" within the MKT Formation aligns with the structural trend observed in the study area, as depicted in Figure 6. The analysis of the drilling lithology indicates that the distribution of these "reversal foresets" shows no direct correlation with the lithological content across the area. However, it is notable that zones with elevated clastic rock and limestone content in the drilling data also exhibit a

predominant NE-SW strike (Figure 6). Consequently, the seismic facies characteristics of the MKT Formation demonstrate similarities with those of deep-water traction current deposits.

The MKT Formation is observed to be an element of a northeast-oriented strip mound deposition (Figure 6), bearing a striking resemblance to the depositional body associated with deep-water traction currents, showcasing a landward migration feature [18,25–27]. On the northwest-strike section, this formation presents a semi-mound shape with a shorter extension, revealing an interior configuration of westward-dipping "reversal foresets" (Figure 6A,B). Conversely, in the northeast-strike section, it adopts a semi-mound shape with a longer extension, displaying a thickness decrease from north (the thickest part) to south. Moreover, the inner strata exhibit a gradual transition from a nearly horizontal reflection to a slow downdip convergence (Figure 6C).

The deep-water traction currents of the MKT Formation, influenced by the formation's substantial scale, and even global variations in sea water temperature, salinity, and density, typically operate over broader ranges and frequently generate larger-scale depositional bodies. For instance, the modern contourite mounds found around the North Atlantic Ocean extend over considerable distances, spanning hundreds of kilometers in length and tens of kilometers in width. In various locations, such as the South China Sea and the Mozambique Basin in the Indian Ocean, deposits related to deep-water traction currents frequently span areas ranging from tens to hundreds of square kilometers [27,28]. Hence, the scale of the MKT Formation bears similarities to that of deposits associated with deep-water traction currents.

Overall, the MKT Formation deposit aligns with the characteristics of deep-water traction current deposits in terms of lithology, form, scale, and seismic facies. Furthermore, the "reversal foreset" configuration, resulting from the inward migration of sediments under the influence of deep-water traction currents, stands out as a distinctive sedimentary feature and serves as a key marker for identifying such deposits.

5. Discussion

5.1. Sedimentary Environment

A contour current refers to consistent and stable water circulation aligned with the ocean's isobaths, resulting from the Earth's rotation and variations in temperature and salinity within the seawater [29–31]. Geologists have discovered numerous ancient deep-water traction current deposits in exposed rock formations since the 1960s [11,29,32–35]. In the past decade, advancements in marine scientific research have led to the successive discovery of numerous modern deep-water traction current deposits both domestically and internationally. Previous research has highlighted the prevalence of the "reversal foreset" configuration in fine sediments, identifying it as a distinctive and widespread sedimentary characteristic of deep-water traction current deposits [36–40].

Deep-water traction current deposits are primarily found in shelf, slope, and oceanic basin regions characterized by considerable water depth. Due to their considerable distance from the source area, these deposits typically consist of mudstone with intermittent layers of thin siltstone and sandstone [36,37]. The MKT Formation, aligning with these deep-water traction currents, comprises extensive layers of dark-gray mudstone interspersed with occasional thin fine siltstone and limestone strata, with an average mudstone content of approximately 78%.

Due to their comparable lithology, form, scale, sedimentary environment, sequence, and contact relationships, differentiating contour current deposits relies on subtle features like bedding type, biological disturbance characteristics, and trace and microfossil details. Utilizing 3D seismic data and drilling well information, this study compares the MKT Formation, identified as a deep-water traction current deposit, with conventional deep-water traction current deposits from various macroscopic aspects (Table 1).

Table 1. Macroscopic feature comparison of MKT Formation and deep-water traction current deposits.

	Lithology	Geographic Setting	Water Setting	Seismic Facies	Foreset Distribution	Configuration	Scale
MKT Fm.	Mudstone and small amount of sandstone and limestone	Shelf slope	Fast water intrusion, deeper water body	Lithology is not related to reversal foreset	Parallel to shelf slope (tectonic line)	In incomplete mound shape (limited by data)	2500 km²
Deep-water traction current deposit	Terrestrial clastic rock and carbonate rock, but mostly mudstone	Shelf, slope, and deep basin	Deeper water body	Lithology is not related to reversal foreset	Generally parallel to slope and basin margin (tectonic line)	In sheet or mound forms	Up to 3000 km²

The sedimentary conditions and environments of the MKT Formation coincide significantly with those of deep-water traction currents. Generally, these deposits tend to develop during periods of substantial regional water depth increase, resulting in a weakened gravity flow effect. In the case of the MKT Formation, the presence of well-developed deep-water mudstone, and the abrupt contact of its bottom with the thick limestone of KT-II (Figures 2 and 3), suggests a rapid subsidence process in the southeastern margin of the basin during the formation's sedimentary period. This environmental shift, transitioning from the high-energy, shallow-water setting of the open platform during the early stage (KT-II) to deeper-water conditions, persisted throughout the deposition of the MKT Formation.

Deep-water traction current deposits are frequently observed in deep-water shelves, slopes, and deep ocean basins, with extensive occurrences predominantly found in the zones of deep-water shelves and slopes [31]. The deep-water traction current deposits within our study area typically feature varying quantities of thin fine sandstone and siltstone interlayers embedded within thick mudstone [41].

During the late Carboniferous Moscovian period, frequent collisions occurred between the East Europe Craton and the Kazakhstan plate, initiating the closure of the Ural Ocean. Consequently, the southeastern margin of the basin underwent a transition from a passive continental margin to a back-arc basin. The sedimentary environment was characterized by alternating neritic platform and shelf-slope settings in the M block. During the deposition of the MKT Formation in the middle Moscovian period, the southeastern part of the basin experienced significant subsidence, resulting in rapid deepening of the water body. This led to the contraction of the platform facies and the expansion of the continental slope facies toward the east and south of the Zanarol uplift zone [6–10,42]. The persistent extension of the slope zone, coupled with deeper-water conditions and a relatively lower-energy environment isolated from shallow waters, emphasized the prominence of deep-water traction currents as the primary agent governing sedimentation.

5.2. "Reversal Foreset Layer" in Sergipe Basin in Brazil

The MKT Formation in the M block was mainly deposited in the deep-water shelf. Morphologically, the "reversal foreset wedge" observed in the MKT Formation closely resembles the continental slope found in the Sergipe Basin in Brazil [43–46] (Figure 7). The structure comprises three west-dipping wedges, reaching thicknesses of up to 1400 m, extending laterally by 15–20 km, and covering an area of 200–400 km² each. The "reversal foreset wedge" exhibits a low-frequency, a weak–medium amplitude, and poor chaotic continuity in the seismic section. Thus, it is inferred that it shares lithological similarities with the MKT Formation, primarily comprising deep-water mudstone, albeit with a more significant presence of clastic and limestone thin beds compared to the MKT Formation.
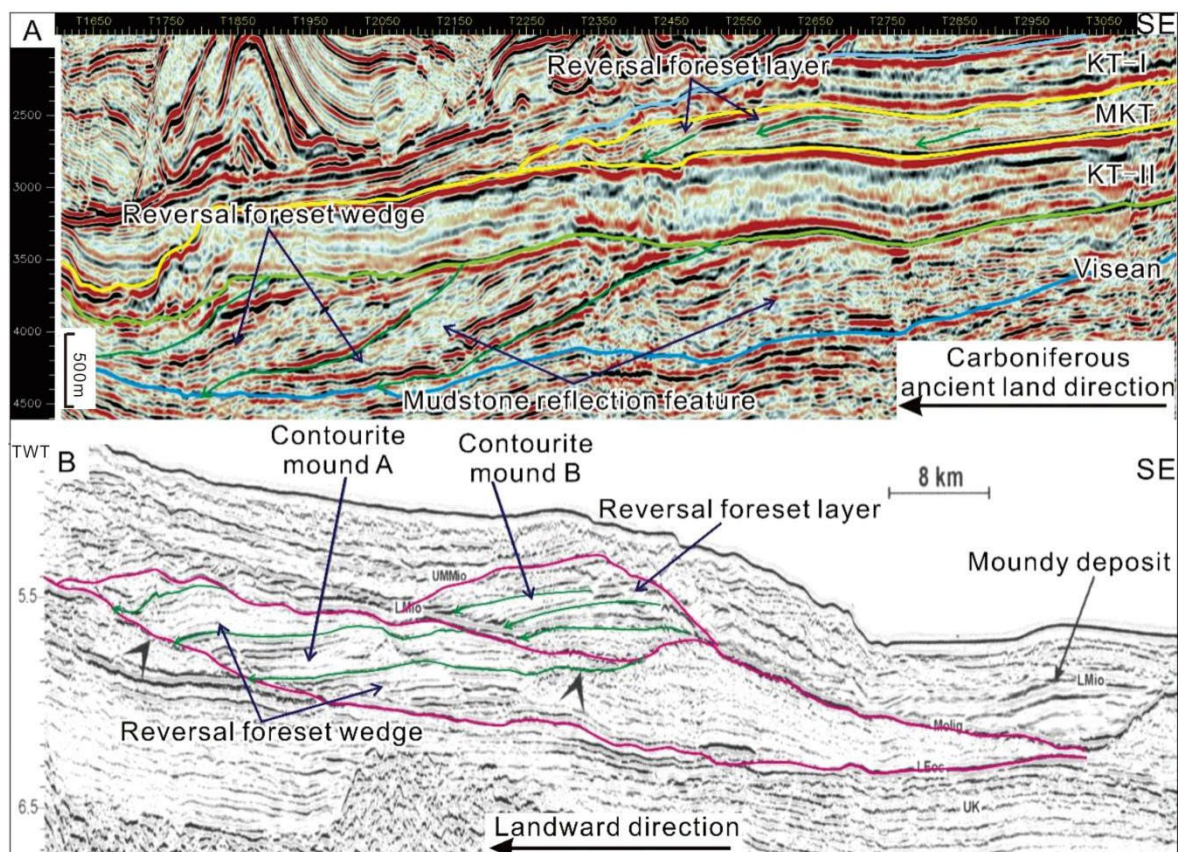
Figure 7. Section of Line Y in study area (**A**) and deep-water traction current deposits in Brazil's Sergipe Basin (**B**). Figure 7B is modified from reference [43]. TWT—two-way travel time.

5.3. Forming Mechanism of "Reversal Foreset"

Deep-water traction current deposits result from the reworking and redeposition of loose sediments from earlier or concurrent periods. While contour currents can generate a "reversal foreset" configuration in sediments, they do so through distinct mechanisms.

The formation of a "reversal foreset" in contour current deposits occurs when the rotational flow of a contour current, influenced by the Coriolis force, disturbs and elevates sediments along the continental slope, creating a "nepheloid layer" mainly composed of fine clay particles. This layer drifts across the sea water density surface toward the oceanic basin side (Figure 8(A-1)). As the "nepheloid layer" gathers an abundance of clay particles, owing to intense suspension and a low deposition rate, these particles travel considerable distances along the density surface towards the basin, forming extensive and flat sheet mudstone deposits. However, if the "nepheloid layer" contains denser grains, like fine-silty sand or limy particles, its suspension ability decreases, leading to a notable rise in the overall sedimentation rate and reduced lateral drift along the density surface. When the water body deepens and the contour current moves towards the land, a new "nepheloid layer" with a swifter deposition rate emerges, drifting over shorter distances and struggling to cover the earlier "nepheloid layer" accumulation completely. Consequently, its sediments predominantly overlay the landward side of the prior "nepheloid layer" accumulation, generating a sequence of landward-migrating "reversal foreset" layers (wedges) (Figure 8(A-2)).

The "reversal foreset" configuration is formed when the body of water deepens, and a contour current is established. In this process, the high-density water layer near the bottom of the deposit on the shelf's slope belt generates internal waves that create a bottom current moving from deeper water to shallower water. These bottom current influences loose sediment, shaping a sedimentary bottom akin to the internal wave, and migrates upward

along the slope, resulting in the establishment of the "reversal foreset" configuration [47] (Figure 8(B-1)–(B-4)).
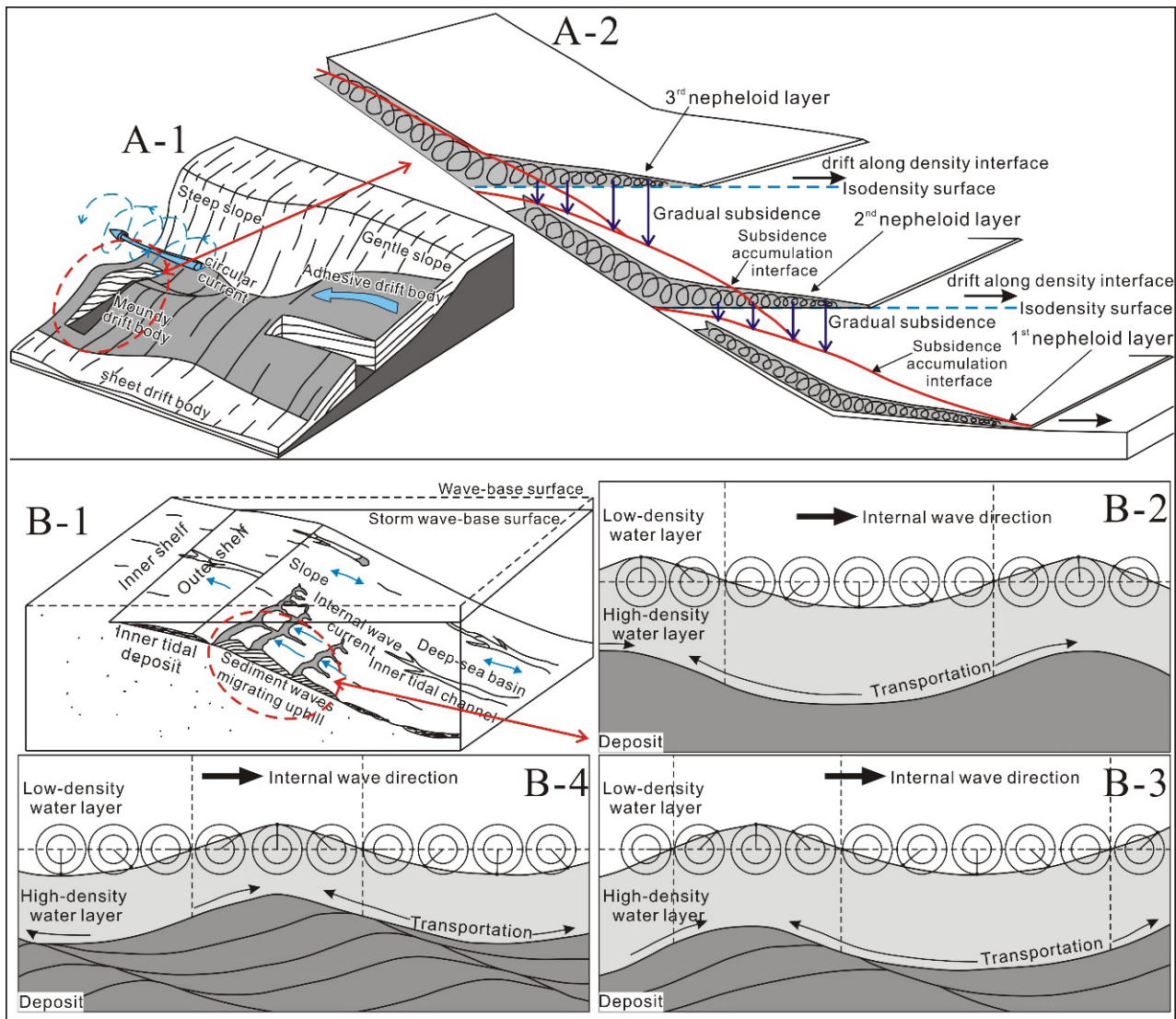

Figure 8. Forming mechanisms of "reversal foresets" in deep-water traction current deposits. (**A**) Sedimentary progress of contourite, modified from reference [48]; (**A-1**): The deep-sea current is a stable circulation formed by the rotation of the Earth and differences in temperature and salinity of seawater. Its landward migration manifests as the formation of spiral flow under the Coriolis effect, which erodes and lifts loose sediments on the landward side to form a misty layer. (**A-2**): During the drifting process along different seawater density layers towards the ocean basin side, gradual sedimentation occurs. When there are small amounts of larger particles such as fine silt in the misty layer, the distance of drift decreases, accelerating the overall sedimentation rate and forming a series of "reverse foresets" migrating towards the land. (**B**) sedimentary progress of internal wave, modified from reference [43]. (**B-1**): Sedimentary bedforms migrate landward, resulting in a series of "reverse foresets". (**B-2**–**B-4**): The bottom current induced by internal waves is opposite to their propagation direction (internal waves typically propagate from shallow water to deep water), causing loose sediments to form sedimentary bedforms of comparable scale to the internal wave morphology without suspension occurring, and gradually migrating landward. This process results in a series of "reverse foresets".

As deep currents exhibit a high degree of consistency in their development environment and conditions [3], their associated sediments often display striking similarities in form and scale. Distinguishing between these deposits primarily relies on more intricate sedimentary data like cores, thin sections, and fossils. Additionally, within the realm of the large-scale development of deep-water traction current sediments, the relationship between internal waves and contour currents remains a matter of debate in academia. Consequently, this study can assert that the upper sections of the MKT are deep-water traction current deposits; however, more detailed refinement of this determination necessitates further information in subsequent research.

6. Conclusions

(1) The MKT Formation primarily consists of shale with interbedded thin siltstone layers. These thin siltstone beds represent deposits formed by deep-water traction currents. The identification of Carboniferous deep-water traction current deposits within this study area presents a valuable non-outcropping example from the deep Paleozoic period, holding significant academic research value.

(2) The identification of deep-water traction current deposits adds to the sedimentary diversity within the Pre-Caspian Basin. Additionally, it validates the notion that the southeastern margin of the basin experienced varied water dynamics during the Paleozoic, suggesting that gravity flow might not have been the dominant factor governing subsidence throughout specific periods.

(3) Deep-water traction currents significantly influence sediment restructuring and play a crucial role in oil and gas exploration. The early accumulation of fine sandstone and siltstone in slope zones often creates promising reservoirs following their restructuring. The thick layers of mudstones within deep-water traction current deposits not only serve as favorable source rocks, but also act as seals for the restructured reservoirs. Consequently, areas characterized by siltstone or sandstone deposition during the initial stages followed by the development of deep-water traction current deposits are highly desirable zones for exploring deep-water lithologic reservoirs in the Pre-Caspian Basin.

Author Contributions: Conceptualization, Y.Z.; methodology, H.D.; software, H.Z. and L.G.; writing original draft preparation, Y.Z., H.D. and H.Z.; writing—review and editing, Y.Z. and L.G.; funding acquisition, Y.Z. and L.G. All authors have read and agreed to the published version of the manuscript.

Data Availability Statement: The data are contained within the article.

Conflicts of Interest: Authors Yajun Zhang, Hansong Dai, Huizhen Zhang were employed by the company PetroChina. The remaining authors declare that the research was conducted in the absence of any commercial or financial relationships that could be construed as a potential conflict of interest.

References

1. Liang, H.; Hansong, D.; Xi, Z.; Bin, Z.; Guobin, L. The Origin Analysis of "Reversal Foreset" of Late Carboniferous MKT Formation in Central Block of Pre-Caspian Basin. *IOP Conf. Ser. Earth Environ. Sci.* **2020**, *602*, 012004. [CrossRef]
2. Jamil, M.; Rahman, A.H.A.; Siddiqui, N.A.; Ibrahim, N.A.; Ahmed, N. A Contemporary Review of Sedimentological and Stratigraphic Framework of the Late Paleogene Deep Marine Sedimentary Successions of West Sabah, North-West Borneo. *Bull. Geol. Soc. Malays.* **2020**, *69*, 53–65. [CrossRef]
3. Jamil, M.; Siddiqui, N.A.; Ahmed, N.; Usman, M.; Umar, M.; Rahim, H.U.; Imran, Q.S. Facies Analysis and Sedimentary Architecture of Hybrid Event Beds in Submarine Lobes: Insights from the Crocker Fan, NW Borneo, Malaysia. *J. Mar. Sci. Eng.* **2021**, *9*, 1133. [CrossRef]
4. Jamil, M.; Siddiqui, N.A.; Usman, M.; Wahid, A.; Umar, M.; Ahmed, N.; Haq, I.U.; El-Ghali, M.A.K.; Imran, Q.S.; Rahman, A.H.A.; et al. Facies Analysis and Distribution of Late Palaeogene Deep-Water Massive Sandstones in Submarine-Fan Lobes, NW Borneo. *Geol. J.* **2022**, *57*, 4489–4507. [CrossRef]

5. Jamil, M.; Siddiqui, N.A.; Umar, M.; Usman, M.; Ahmed, N.; Rahman, A.H.A.; Zaidi, F.K. Aseismic and Seismic Impact on Development of Soft-Sediment Deformation Structures in Deep-Marine Sand-Shaly Crocker Fan in Sabah, NW Borneo. *J. King Saud. Univ. Sci.* **2021**, *33*, 101522. [CrossRef]

6. Pu, R.; Su, J.; Yu, R. Progradational Reflections Caused by Shale. *Oil Geophys. Prospect.* **2012**, *47*, 624–628.

7. Mcconnico, T.S.; Bassett, K.N. Gravelly Gilbert-Type Fan Delta on the Conway Coast, New Zealand: Foreset Depositional Processes and Clast Imbrications. *Sediment. Geol.* **2007**, *198*, 147–166. [CrossRef]

8. Shanmugam, G. Deep-Marine Tidal Bottom Currents and Their Reworked Sands in Modern and Ancient Submarine Canyons. *Mar. Petrol. Geol.* **2003**, *20*, 471–491. [CrossRef]

9. Wang, Z.; Fan, R.; Zong, R.; Gong, Y. Composition and Spatiotemporal Evolution of the Mixed Turbidite-Contourite Systems from the Middle Ordovician, in Western Margin of the North China Craton. *Sediment. Geol.* **2021**, *421*, 105943. [CrossRef]

10. Gong, C.; Wang, Y.; Xu, S.; Pickering, K.T.; Peng, X.; Li, W.; Yan, Q. The Northeastern South China Sea Margin Created by the Combined Action of Down-Slope and along-Slope Processes: Processes, Products and Implications for Exploration and Paleoceanography. *Mar. Petrol. Geol.* **2015**, *64*, 233–249. [CrossRef]

11. Shanmugam, G. 150 Years (1872–2022) of Research on Deep-Water Processes, Deposits, Settings, Triggers, and Deformation: A Difficult Domain of Progress, Dichotomy, Diversion, Omission, and Groupthink. *J. Palaeogeogr.* **2022**, *11*, 469–564. [CrossRef]

12. Csato, I.; Homonnai, O.; Zadravecz, C.; Catuneanu, O. Lower Visean Sea-Level Changes in the Northern Precaspian Basin. *Mar. Petrol. Geol.* **2021**, *132*, 105186. [CrossRef]

13. Volozh, Y.A.; Antipov, M.P.; Brunet, M.-F.; Garagash, I.A.; Lobkovskii, L.I.; Cadet, J.-P. Pre-Mesozoic Geodynamics of the Precaspian Basin (Kazakhstan). *Sediment. Geol.* **2003**, *156*, 35–58. [CrossRef]

14. Zhu, X.; Jin, Z.; Liang, T.; Yi, S.; Wei, K.; Gao, B.; Shi, L. Depositional Environment, Diagenetic Evolution, and Their Impact on the Reservoir Quality of the Carboniferous KT-II Carbonate in the Zhanazhol Reservoir, Pre-Caspian Basin, Kazakhstan. *Mar. Petrol. Geol.* **2020**, *117*, 104411. [CrossRef]

15. Ross, C.A.; Ross, J.R.P. Carboniferous and Early Permian Biogeography. *Geology* **1985**, *13*, 27–30. [CrossRef]

16. Zhou, X.; Ding, W.; He, J.; Li, A.; Sun, Y.; Wang, X. Microfractures in the Middle Carboniferous Carbonate Rocks and Their Control on Reservoir Quality in the Zanaral Oilfield. *Mar. Petrol. Geol.* **2018**, *92*, 462–476. [CrossRef]

17. Miao, Q.; Wang, Y.; Zhu, X.; Yu, B.; Jiang, J. Sequence Stratigraphy of Carboniferous in Eastern Margin of Pre-Caspian Basin. *Xinjiang Petrol. Geol.* **2013**, *34*, 483–487.

18. Craig, F.; Carter, R. Continental-Shelf Progradation by Sediment-Drift Accretion. *GSA Bull.* **1991**, *103*, 300–309.

19. He, Y.; Gao, Z. Middle-Upper Ordovician Internal-Wave and Internal-Tide Deposits and Their Significance of Petroleum Geology in the Central Tarim Basin. *Mar. Orig. Petrol. Geol.* **2002**, *7*, 33–40.

20. Taskyn, A.; Li, J.; Li, H.; Li, W.; Mao, X.; Wang, H. Tectonic Evolution and Hydrocarbon Potential of Basins in Central Asia and Its Adjacent Regions. *Geoscience* **2014**, *28*, 573–584.

21. Yu, R. Ancient Structural Evolution of Hydrocarbon Accumulation in Southeastern Part of Gi Ant Synclise of Caspian Seashore Basin (Translated by REN YU). *Xinjiang Petrol. Geol.* **2002**, *23*, 351–354.

22. Dickson, J.A.D.; Kenter, J.A.M. Diagenetic Evolution of Selected Parasequences Across A Carbonate Platform: Late Paleozoic, Tengiz Reservoir, Kazakhstan. *J. Sediment. Res.* **2014**, *84*, 664–693. [CrossRef]

23. Faugeres, J.C.; Gonthier, E.; Grousset, F.; Poutiers, J. The Feni Drift: The Importance and Meaning of Slump Deposits on the Eastern Slope of the Rockall Bank. *Mar. Geol.* **1981**, *40*, 49–57. [CrossRef]

24. Haq, B.; Schutter, S.R. A Chronology of Paleozoic Sea-Level Changes. *Science* **2008**, *322*, 64–68. [CrossRef] [PubMed]

25. Gao, Z.; Peng, D.; Liu, X.; He, Y.; Fu, X.; Li, D.; Zhong, G. Ordovician Internal-Tide Deposits in TZ30 Well, Tarim Basin. *J. Jianghan Petrol. Insititute* **1996**, *18*, 9–14.

26. De Hass, H.; Van Weering, T.; Stoker, M.S. *Development of a Sediment Drift: Feni Drift, NE Atlantic Margin*; Springer: Berlin/Heidelberg, Germany, 2003; pp. 197–201.

27. Liu, L. Characteristics and Research Status of Deep Water Traction Current Deposits. *Oil Gas. Geol.* **1999**, *20*, 369–374.

28. Wang, Q.; Bao, Z.; He, P. Forms of Internal Wave and Internal Tide Sedimentation. *Mar. Geol. Lett.* **2005**, *21*, 10–13.

29. Ahmed Zaib, M.; Waqar, A.; Abbas, S.; Badshah, S.; Ahmad, S.; Amjad, M.; Rahimian Koloor, S.S.; Eldessouki, M. Effect of Blade Diameter on the Performance of Horizontal-Axis Ocean Current Turbine. *Energies* **2022**, *15*, 5323. [CrossRef]

30. Batchelor, C.L.; Bellwald, B.; Planke, S.; Ottesen, D.; Henriksen, S.; Myklebust, R.; Johansen, S.E.; Dowdeswell, J.A. Glacial, Fluvial and Contour-Current-Derived Sedimentation along the Northern North Sea Margin through the Quaternary. *Earth Planet. Sci. Lett.* **2021**, *566*, 116966. [CrossRef]

31. Zhao, Y.; Liu, Z.; Zhang, Y.; Li, J.; Wang, M.; Wang, W.; Xu, J. In Situ Observation of Contour Currents in the Northern South China Sea: Applications for Deepwater Sediment Transport. *Earth Planet. Sci. Lett.* **2015**, *430*, 477–485. [CrossRef]

32. Guo, L.; Jia, C.; Du, W. Geochemistry of Lower Silurian Shale of Longmaxi Formation, Southeastern Sichuan Basin, China: Implications for Provenance and Source Weathering. *J. Cent. South Univ.* **2016**, *23*, 669–676. [CrossRef]

33. Guo, L.; Jiang, Z.; Zhang, J.; Li, Y. Paleoenvironment of Lower Silurian Black Shale and Its Significance to the Potential of Shale Gas, Southeast of Chongqing, China. *Energ. Explor. Exploit.* **2011**, *29*, 597–616. [CrossRef]

34. Xian, B.; Wang, J.; Gong, C.; Yin, Y.; Chao, C.; Liu, J.; Zhang, G.; Yan, Q. Classification and Sedimentary Characteristics of Lacustrine Hyperpycnal Channels: Triassic Outcrops in the South Ordos Basin, Central China. *Sediment. Geol.* **2018**, *368*, 68–82. [CrossRef]

35. Yang, T.; Cao, Y.; Liu, K.; Tian, J.; Kneller, B. Depositional Elements and Evolution of Gravity-Flow Deposits on Lingshan Island (Eastern China): An Integrated Outcrop-Subsurface Study. *Mar. Petrol. Geol.* **2022**, *138*, 105566. [CrossRef]

36. Ding, H.; Meng, X.; Ge, M.; Xue, H. Ordovician Contourite of the North Part of Helan Aulacogen. *J. Earth Sci. Environ.* **2009**, *31*, 58–64.

37. He, Y.; Gao, Z.; Li, J. Petrological Characteristics and Sedimentar Environment of the Yankou Formation in Ther Upper Ordovician at Tonglu Area in Zhejiang Province. *J. Palaeogeogr.* **1999**, *1*, 65–71.

38. He, Y.; Gao, Z.; Li, J.; Li, W.; Luo, S.; Wang, Z. Internal-Tide Deposits of the Late Ordovician in Tonglu, Zhejiang. *Acta Sedimentol. Sin.* **1998**, *16*, 1–7.

39. He, Y.; Luo, S.; Gao, Z. The Recent Advances and Prospects of the Study on Deep-Water Tractive Current Deposits. *Adv. Earth Sci.* **1997**, *12*, 247–252.

40. He, Y.B.; Gao, Z.Z.; Guo, C.X.; Xu, H.; Dong, G.Y. Study on Internal-Wave and Internal-Tide Deposits of the Third Member of the Lower Cambrian Balang Formation at Yangjiaping, Shimen. *Chin. Geol.* **2005**, *32*, 66–69.

41. Shanmugam, G. Contourites: Physical Oceanography, Process Sedimentology, and Petroleum Geology. *Petrol. Explor. Dev.* **2017**, *44*, 183–216. [CrossRef]

42. Dai, H.; Chen, B.; Hao, J.; Liu, X.; Hong, L.; Zhao, X.; Deng, G. Nature of "Reverse Prograding Deposits" at the Southeast Margin of Pre-Caspian Basin. *Sediment. Geol.* **2018**, *39*, 1246–1254. [CrossRef]

43. Gomes, P.O.; Viana, A.R. Contour Currents, Sediment Drifts and Abyssal Erosion on the Northeastern Continental Margin off Brazil. *Geol. Soc. Lond. Mem.* **2002**, *22*, 239–248. [CrossRef]

44. Luft-Souza, F.; Fauth, G.; Bruno, M.D.R.; De Lira Mota, M.A.; Vázquez-García, B.; Santos Filho, M.A.B.; Terra, G.J.S. Sergipe-Alagoas Basin, Northeast Brazil: A Reference Basin for Studies on the Early History of the South Atlantic Ocean. *Earth-Sci. Rev.* **2022**, *229*, 104034. [CrossRef]

45. Mohriak, W.U.; Bassetto, M.; Vieira, I.S. Crustal Architecture and Tectonic Evolution of the Sergipe-Alagoas and Jacuípe Basins, Offshore Northeastern Brazil. *Tectonophysics* **1998**, *288*, 199–220. [CrossRef]

46. Pinheiro, J.M.; Schnurle, P.; Evain, M.; Afilhado, A.; Gallais, F.; Klingelhoefer, F.; Loureiro, A.; Fuck, R.; Soares, J.; Cupertino, J.A.; et al. Lithospheric Structuration Onshore-Offshore of the Sergipe-Alagoas Passive Margin, NE Brazil, Based on Wide-Angle Seismic Data. *J. S. Am. Earth Sci.* **2018**, *88*, 649–672. [CrossRef]

47. Wang, Q.; Bao, Z.; He, P. The Generational Mechanism of Orientating Sedimentary Structure by Internal-Waves. *Acta Sedimentol. Sin.* **2005**, *23*, 255–259.

48. Faugères, J.C.; Mulder, T. Contour Currents and Contourite Drifts. *Dev. Sedimentol.* **2011**, *63*, 149–214.